A search for the electroweak production of $Z\gamma$ with two jets and anomalous quartic gauge couplings in pp collisions at $\sqrt{s}$ = 13 TeV

CLHCP 2019, DaLian
Oct 24, 2019

Meng Lu on behalf of EW $Z\gamma$ group

CMS PAS SMP-18-007

Outline

- Introduction and motivation
- Event selection
- Backgrounds estimation
- Data and MC yields
- Uncertainty and EW extraction
- aQGC
- Summary and outlook

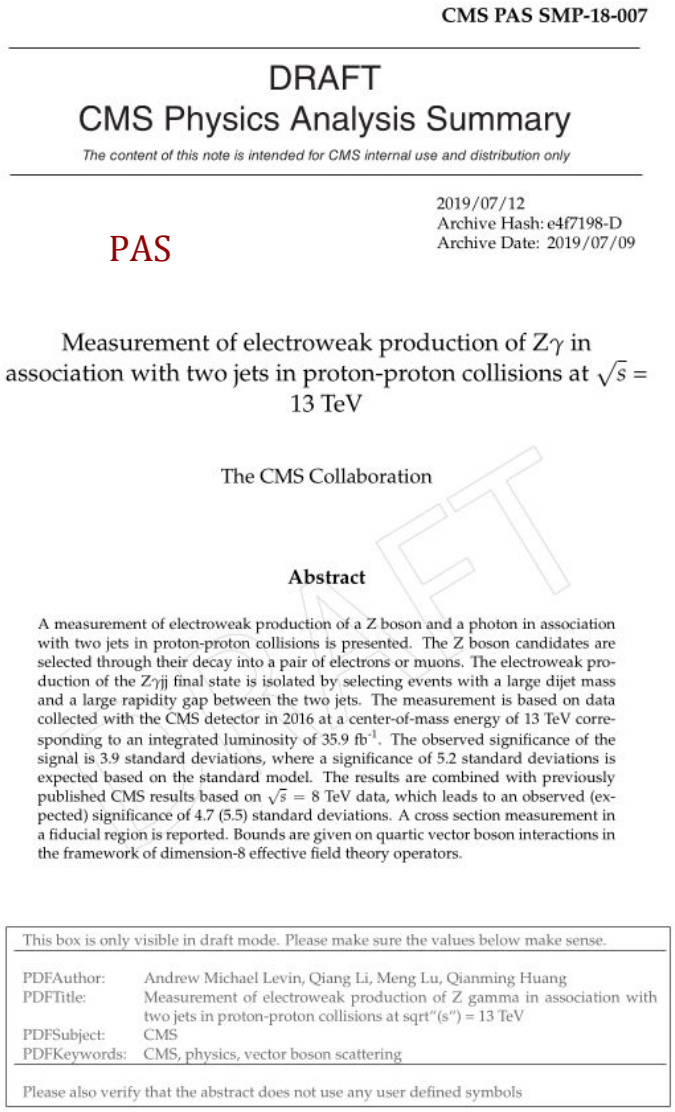

CMS PAS SMP-18-007

DRAFT

CMS Physics Analysis Summary

The content of this note is intended for CMS internal use and distribution only

2019/07/12
Archive Hash: e4f7198-D
Archive Date: 2019/07/09

PAS

Measurement of electroweak production of $Z\gamma$ in association with two jets in proton-proton collisions at $\sqrt{s}$ = 13 TeV

The CMS Collaboration

Abstract

A measurement of electroweak production of a Z boson and a photon in association with two jets in proton-proton collisions is presented. The Z boson candidates are selected through their decay into a pair of electrons or muons. The electroweak production of the $Z\gamma jj$ final state is isolated by selecting events with a large dijet mass and a large rapidity gap between the two jets. The measurement is based on data collected with the CMS detector in 2016 at a center-of-mass energy of 13 TeV corresponding to an integrated luminosity of 35.9 fb^{-1}. The observed significance of the signal is 3.9 standard deviations, where a significance of 5.2 standard deviations is expected based on the standard model. The results are combined with previously published CMS results based on $\sqrt{s}$ = 8 TeV data, which leads to an observed (expected) significance of 4.7 (5.5) standard deviations. A cross section measurement in a fiducial region is reported. Bounds are given on quartic vector boson interactions in the framework of dimension-8 effective field theory operators.

This box is only visible in draft mode. Please make sure the values below make sense.

PDFAuthor:	Andrew Michael Levin, Qiang Li, Meng Lu, Qianming Huang
PDFTitle:	Measurement of electroweak production of Z gamma in association with two jets in proton-proton collisions at sqrt"(s") = 13 TeV
PDFSubject:	CMS
PDFKeywords:	CMS, physics, vector boson scattering

Please also verify that the abstract does not use any user defined symbols

Introduction and motivation

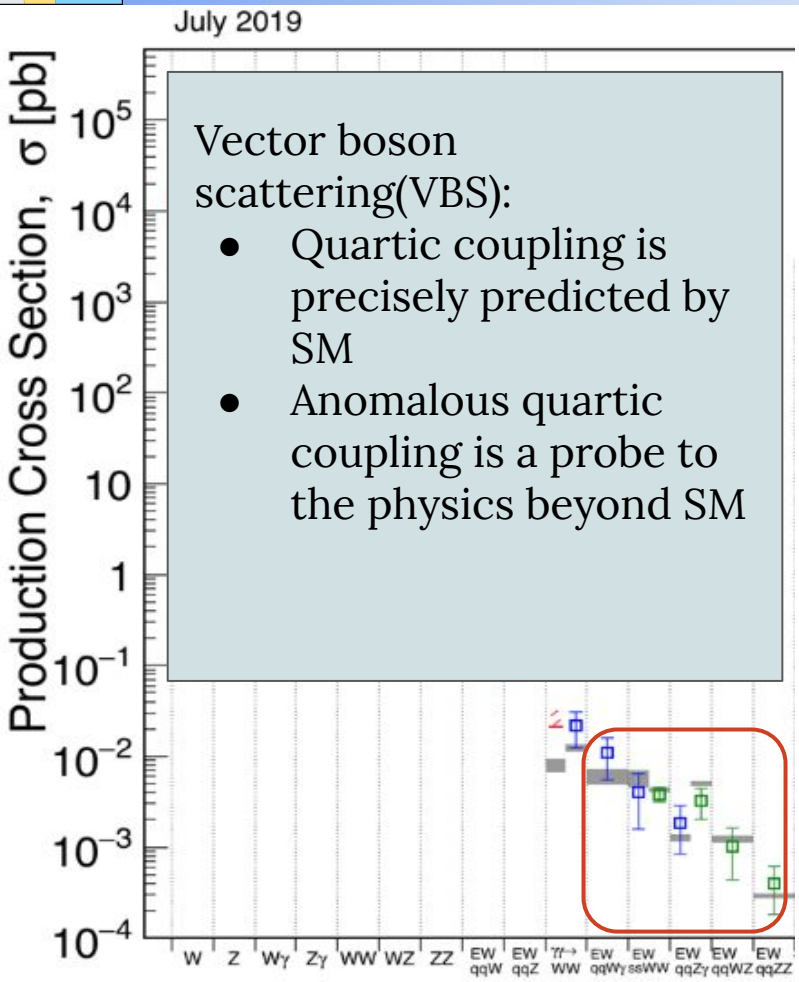

Vector boson scattering(VBS):

- Quartic coupling is precisely predicted by SM
- Anomalous quartic coupling is a probe to the physics beyond SM

Zγ analysis include:

- EWK production of Z boson and photon
- Irreducible QCD production with same final state

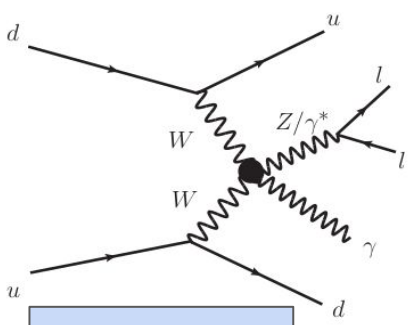

EWK signal

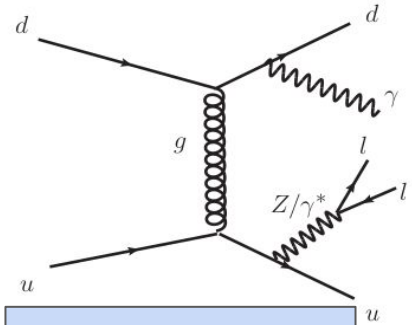

QCD Background

RunI: 3σ evidence

RunII: observed(expected) 3.9(5.2)σ

- 5σ measurement of VBS di-boson in ssWW with 2016 data by CMS and ATALS, VBS WZ by ATLAS, VBS ZZ was discovered by ATLAS with full RunII dataset.
- Several full RunII VBS analysis ongoing in both CMS and ATLAS

Event selection

- Two and only two same-flavor good leptons
- Third lepton veto
- One good photon with pT > 20 GeV
- Two jets with pT > 30 GeV
- 70 GeV < M_{ll} < 110 GeV

Basic event selection

- $M_{ll\gamma}$ > 100 GeV

Suppress FSR

- 150 GeV < M_{jj} < 400 GeV

Low M_{jj} control region

- M_{jj} > 500 GeV
- $\Delta\eta(j_1, j_2) > 2.5$

VBS signal region

- Zepp = $|\eta_{Z\gamma} - (\eta_{j1} + \eta_{j2})/2| < 2.4$
- dphi = $|\phi_{Z\gamma} - \phi_{j1,j2}| > 1.9$

For EW signal extraction

Optimization has been performed on Zepp and dphi to extract the EW signal process

Backgrounds estimation

The following processes have same final status with signal process, the contribution is estimated in VBS region

Category	Estimation method	contribution
QCD Zγ	From simulation	~56%
Fake photon	From template fit method, data-driven	~40%
di-boson	From simulation	~2%
TTγ	From simulation	~2%
Single-Top	From simulation	<1%
Wγ	From simulation	~0%

QCD Zγ and fake photon are the two largest backgrounds.
Pile-up weights are applied while simulations are used

Backgrounds estimation: fake photon estimation

Photon in jets(mainly comes from neutral meson decay) could be identified as good photon.

region D: cut-based medium photon
Goal: estimate fake photon fraction in region D.

region A+B: charged isolation far away from medium value, mainly fake photon candidates.

Charged isolation and $\sigma i\eta i\eta$ are weakly correlated

$\sigma i\eta i\eta$ distribution of fake photon in region D+C could be approximated from region A+B

region D+C: mixed $\sigma i\eta i\eta$ distribution of true photon and fake photon in datasets.

$\sigma i\eta i\eta$ distribution of true photon in region D+C could be obtained from MC sample by using MC truth information.

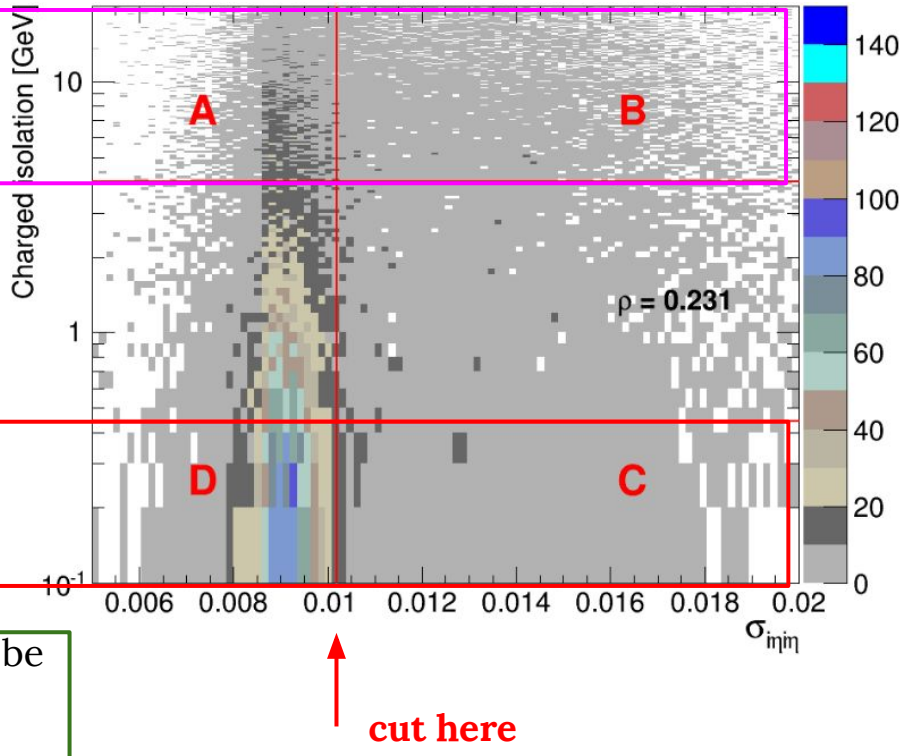

Using $\sigma i\eta i\eta$ shape of true photon and fake photon to do fit on the $\sigma i\eta i\eta$ shape of data, then apply medium ID's $\sigma i\eta i\eta$ cut to extract **fake photo fraction in region D**.

Backgrounds estimation: fake photon estimation

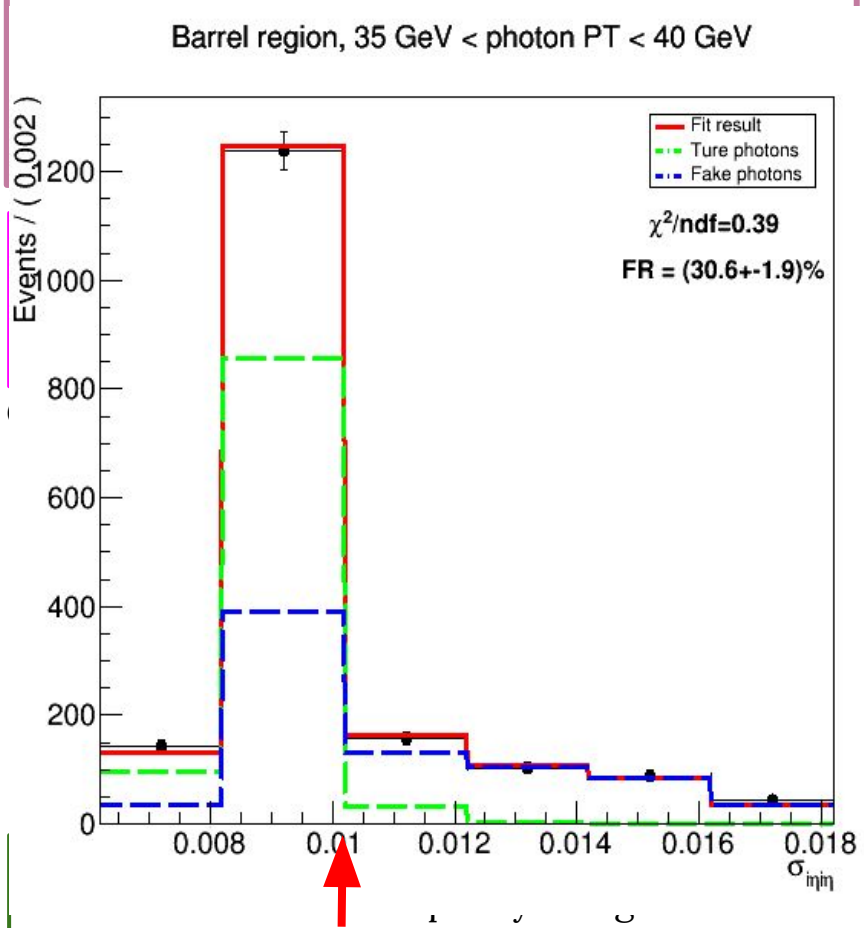

information.

region D: cut-based medium photon

Goal: estimate fake photon fraction in region D.

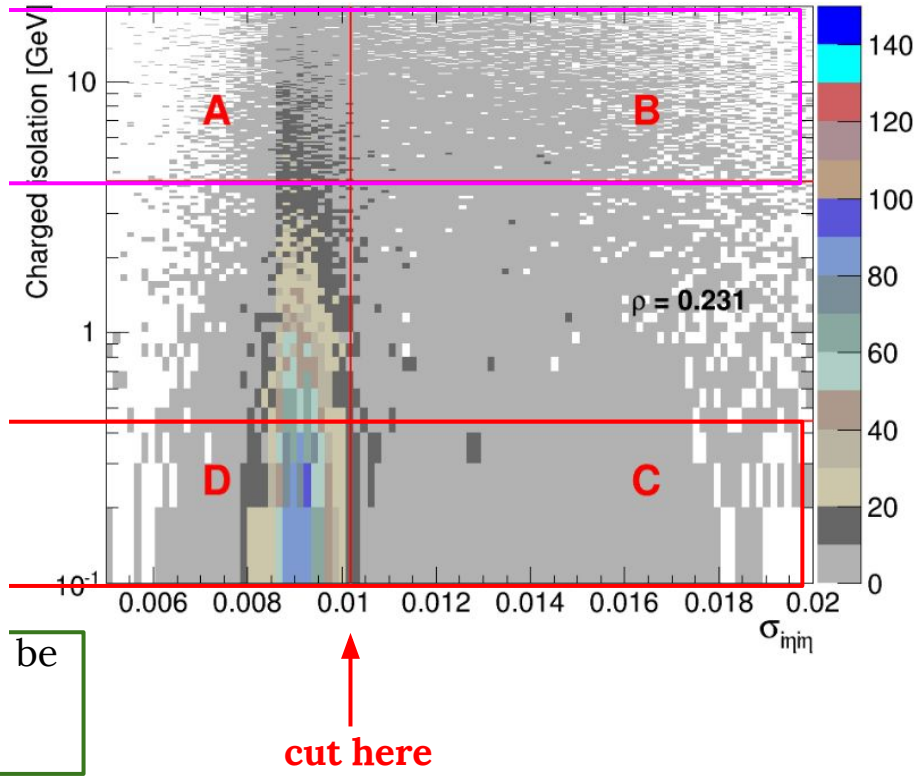

be

Using $\sigma i\eta i\eta$ shape of true photon and fake photon to do fit on the $\sigma i\eta i\eta$ shape of data, then apply medium ID's $\sigma i\eta i\eta$ cut to extract **fake photo fraction in region D**.

Backgrounds estimation: PLJ sample

A fake photon enrich sample is needed, we call it 'medium-photon-like' jets sample, i.e. PLJ sample, it's from data sample.

Apply the medium photon ID cuts to all variables but one, variable X, and apply the inverted loose photon ID cut to variable X
(inverse chiso while keep others medium) ||
(inverse sieie while keep others medium) ||
(inverse nhiso while keep others medium) ||
(inverse phoiso while keep others medium)

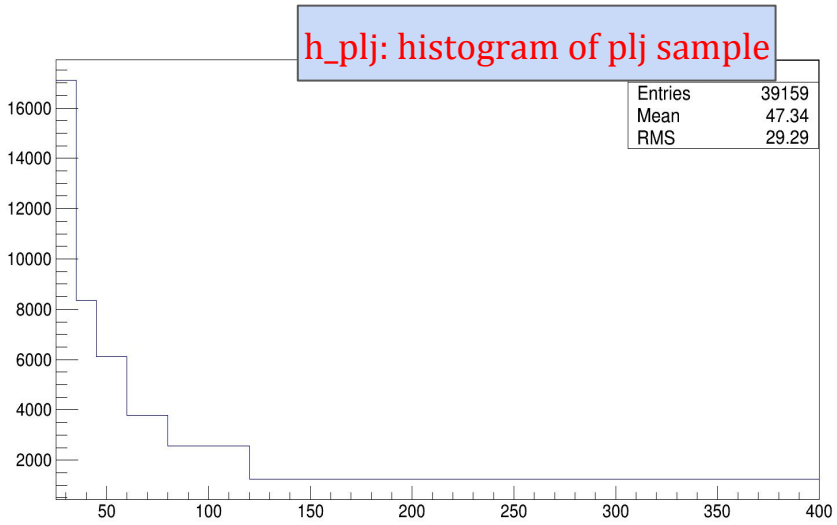

For each event in PLJ sample, a weight is applied w.r.t the photon pT,

$$W_{p_T^\gamma} = \frac{h_{data} \rightarrow GetBinContent(p_T^\gamma)}{h_{plj} \rightarrow GetBinContent(p_T^\gamma)} * fake\_fraction_{p_T^\gamma},$$

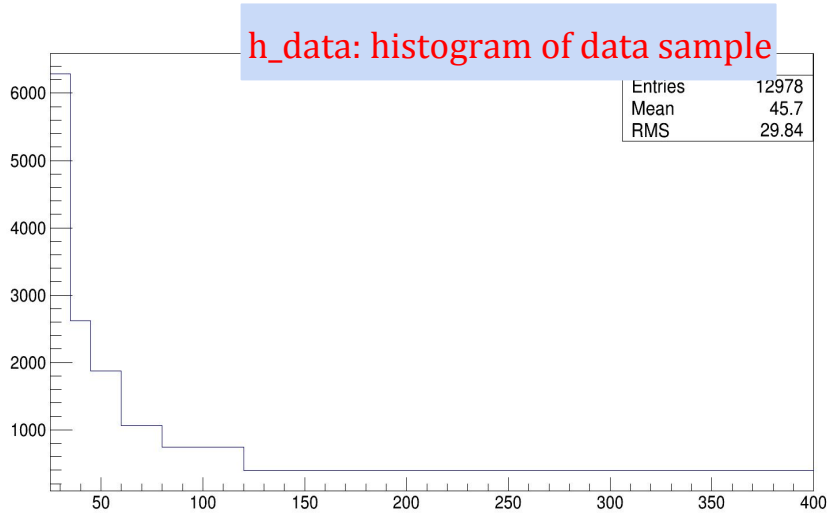

Data and MC yields

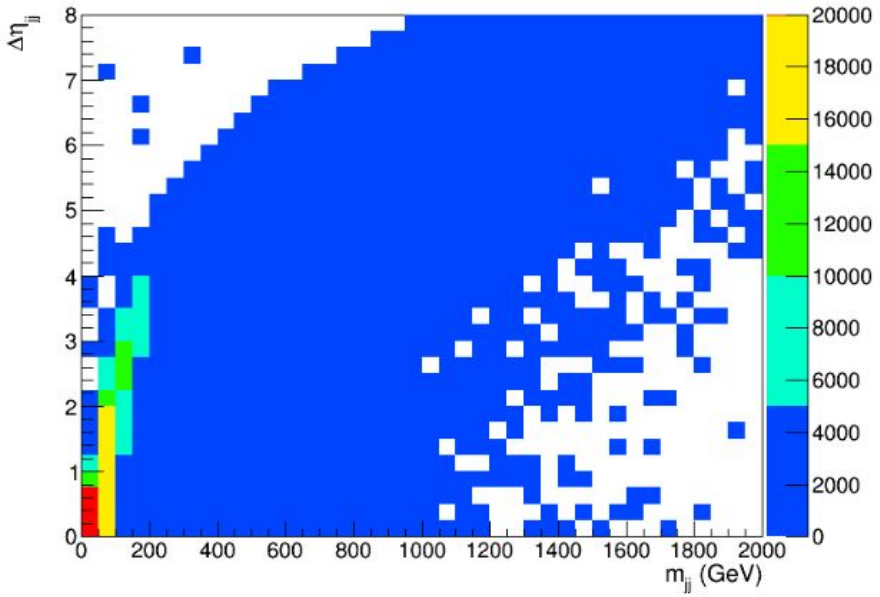

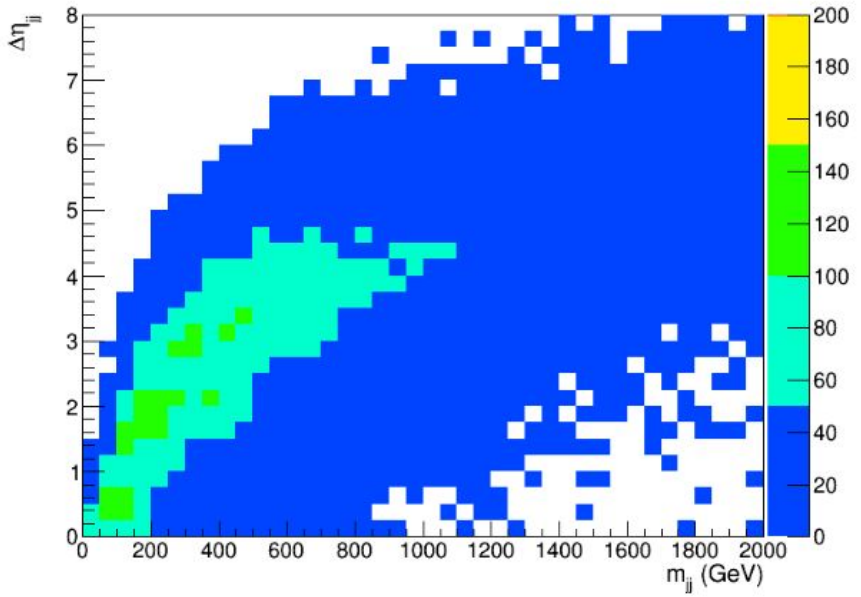

Dijet mass and η separation of two jets for QCD Zγ+jets(left) and EWK signal(right), different behaviour shown in the plots. Simultaneously 2D distributions of Mjj and $\Delta\eta$(j1, j2).

Mjj ~ [500, 800, 1200, inf]

$\Delta\eta$(j1, j2) ~ [2.5, 4.5, 6, inf]

Scan on zepp and dphi →

- Zepp = $|\eta_{Z\gamma} - (\eta_{j1} + \eta_{j2})/2| < 2.4$
- dphi = $|\phi_{Z\gamma} - \phi_{j1,j2}| > 1.9$

Data and MC yields

	muon channel	electron channel
Nonprompt photon	47.6 ± 4.5	39.3 ± 4.0
Other background	7.4 ± 1.4	2.7 ± 0.8
QCD $Z\gamma jj$	62.9 ± 3.1	49.6 ± 2.7
EW $Z\gamma jj$	36.5 ± 0.7	25.4 ± 0.6
Total background	117.9 ± 5.6	91.6 ± 4.8
Data	172 ± 13	113 ± 11

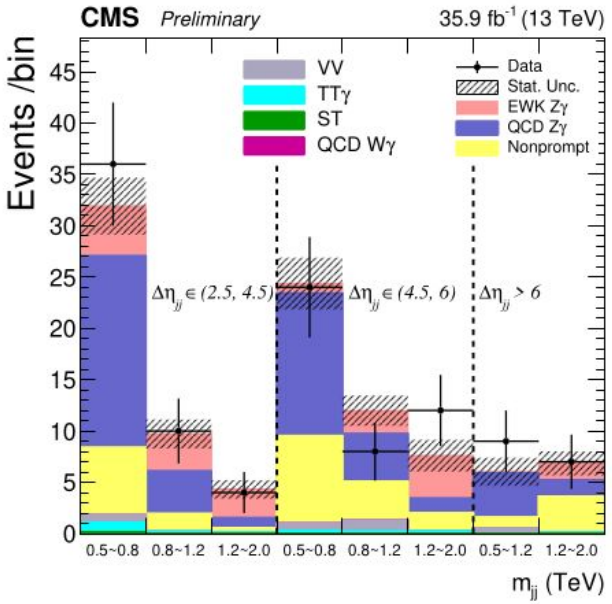

PAS

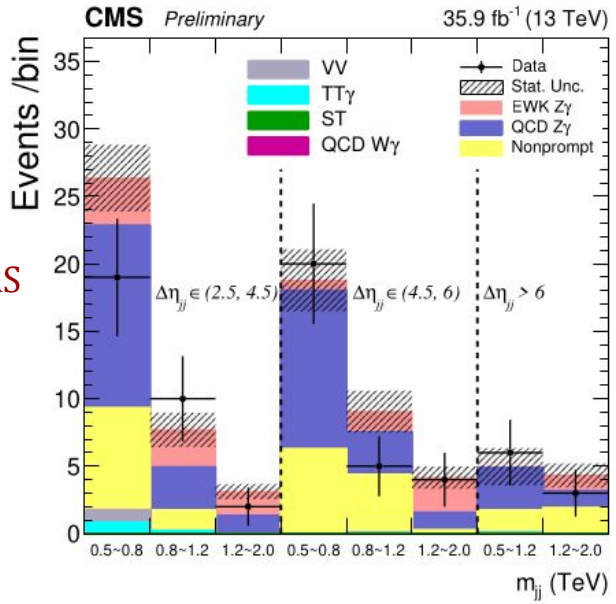

Just barrel photon

Uncertainty estimation

Source of systematic uncertainty	Relative uncertainty [%]
QCD $Z\gamma$ scale	5 - 25
EW $Z\gamma$ scale	2 - 14
JES	1 - 31
JER	1 - 13
Interference	4 - 8
Nonprompt photon	9 - 37
Integrated luminosity	2.5

Pre-fit dominant uncertainties, while the QCD $Z\gamma$ is the largest one. It's constrained by using a simultaneous fit of control region and signal region.

Result: significance and cross section

Significance: 2016 only, observed(expected), 3.9(5.2)
Combine 8TeV: observed(expected), 4.7(5.5)

Signal strength: 0.64+-0.23
Fiducial cross section:

$$\sigma_{\mathrm{EW}}^{\mathrm{fid}} = 3.20 \pm 0.07\,(\mathrm{lumi}) \pm 1.00\,(\mathrm{stat}) \pm 0.57\,(\mathrm{syst})\ \mathrm{fb} = 3.20 \pm 1.15\ \mathrm{fb}.$$

$$4.97 \pm 0.25\,(\mathrm{scale}) \pm 0.14\,(\mathrm{PDF})\ \mathrm{fb}$$

QCD+EW Signal strength: 0.96+-0.15
Fiducial cross section:

$$\sigma_{\mathrm{EW+QCD}}^{\mathrm{fid}} = 15.1 \pm 0.5\,(\mathrm{lumi}) \pm 1.2\,(\mathrm{stat}) \pm 2.1\,(\mathrm{syst})\ \mathrm{fb} = 15.1 \pm 2.5\ \mathrm{fb}$$

$$15.7 \pm 1.7\,(\mathrm{scale}) \pm 0.2\,(\mathrm{PDF})\ \mathrm{fb}$$

aQGC estimation: theoretical part

- Generic parametrization of a hidden theory at larger energy scales than the current experimental reach
- SM lagrangian can be extended with higher dimensional operators
  remaining SU(2)×U(1) gauge symmetry

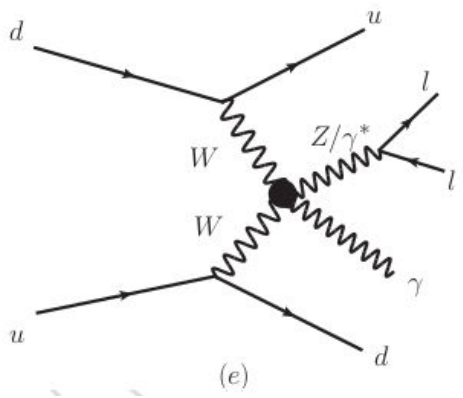

$$\mathcal{L}_{\text{eff}} = \mathcal{L}_{\text{SM}} + \sum_{n=5}^{\infty} \frac{f_n}{\Lambda^{n-4}} \mathcal{O}_n$$

Set of dim-8 operators affecting quartic boson vertices

	WWWW	WWZZ	ZZZZ	WWAZ	WWAA	ZZZA	ZZAA	ZAAA	AAAA
$\mathcal{L}_{S,0}$, $\mathcal{L}_{S,1}$	X	X	X	O	O	O	O	O	O
$\mathcal{L}_{M,0}$, $\mathcal{L}_{M,1}$,$\mathcal{L}_{M,6}$,$\mathcal{L}_{M,7}$	X	X	X	X	X	X	X	O	O
$\mathcal{L}_{M,2}$,$\mathcal{L}_{M,3}$, $\mathcal{L}_{M,4}$,$\mathcal{L}_{M,5}$	O	X	X	X	X	X	X	O	O
$\mathcal{L}_{T,0}$,$\mathcal{L}_{T,1}$,$\mathcal{L}_{T,2}$	X	X	X	X	X	X	X	X	X
$\mathcal{L}_{T,5}$,$\mathcal{L}_{T,6}$,$\mathcal{L}_{T,7}$	O	X	X	X	X	X	X	X	X
$\mathcal{L}_{T,9}$,$\mathcal{L}_{T,9}$	O	O	X	O	O	X	X	X	X

aQGC estimation

Use MadGraph5_aMC@NLO at LO with reweighing to different parameter points(16 points for each parameter) for each operator with sensitivity.

- $p_{\mathrm{T}}^{j1,j2} > 30$ GeV, $|\eta^{j1,j2}| < 4.7$
- $M_{jj} > 500$ GeV, $\Delta\eta_{jj} > 2.5$
- $p_{T}^{l1,l2} > 20(25)$ GeV, $|\eta^{l1,l2}| < 2.4(2.5)$, muon(electron)
- $70\ \mathrm{GeV} < M_{ll} < 110\ \mathrm{GeV}$
- $p_{T}^{\gamma} > 100$ GeV, $|\eta^{\gamma}| < 1.4442$ or $1.566 < |\eta^{\gamma}| < 2.5$
- $\Delta R_{jj}, \Delta R_{j\gamma}, \Delta R_{jl} > 0.5, \Delta R_{l\gamma} > 0.7$

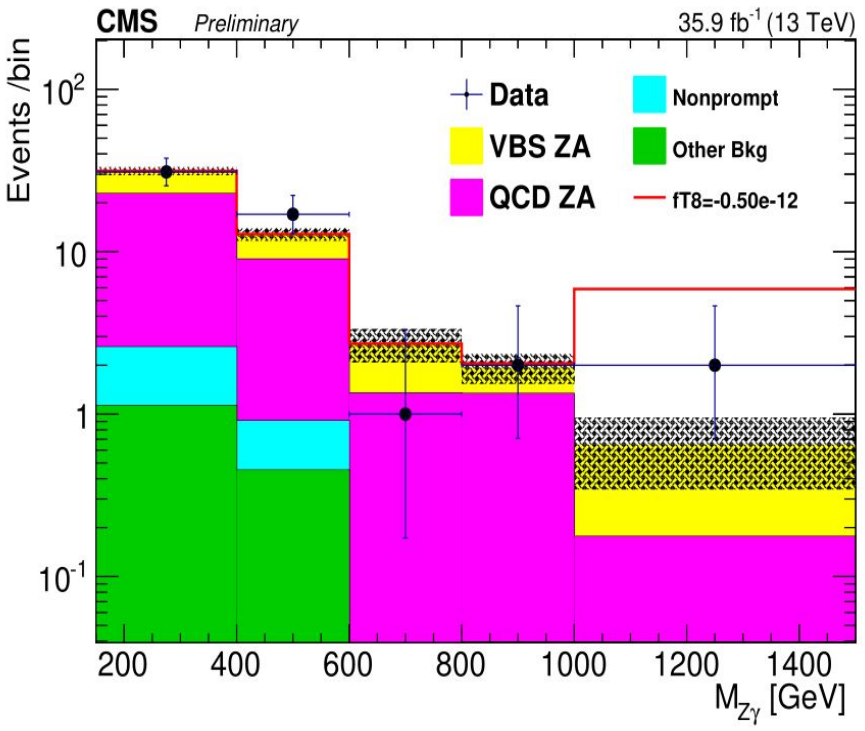

Limits are estimated based on ATGCRooStats, using ZGmass to obtain limits, ZGmass[6]= {150,400,600,800, 1000, infi}

aQGC estimation: limits

Observed Limits (TeV^{-4})	Expected Limits (TeV^{-4})	Unitarity Bound
$-19.3 < F_{M,0}/\Lambda^4 < 20.2$	$-15.0 < F_{M,0}/\Lambda^4 < 15.1$	1.0
$-47.8 < F_{M,1}/\Lambda^4 < 46.9$	$-30.1 < F_{M,1}/\Lambda^4 < 30.0$	1.2
$-8.16 < F_{M,2}/\Lambda^4 < 8.04$	$-6.09 < F_{M,2}/\Lambda^4 < 6.06$	1.3
$-20.9 < F_{M,3}/\Lambda^4 < 21.1$	$-13.2 < F_{M,3}/\Lambda^4 < 13.3$	1.5
$-15.2 < F_{M,4}/\Lambda^4 < 15.8$	$-11.7 < F_{M,4}/\Lambda^4 < 11.7$	1.5
$-24.9 < F_{M,5}/\Lambda^4 < 24.4$	$-19.1 < F_{M,5}/\Lambda^4 < 18.2$	1.8
$-38.6 < F_{M,6}/\Lambda^4 < 40.5$	$-30.0 < F_{M,6}/\Lambda^4 < 30.1$	1.0
$-60.8 < F_{M,7}/\Lambda^4 < 62.6$	$-46.1 < F_{M,7}/\Lambda^4 < 46.3$	1.3
$-0.74 < F_{T,0}/\Lambda^4 < 0.69$	$-0.56 < F_{T,0}/\Lambda^4 < 0.51$	1.4
$-1.16 < F_{T,1}/\Lambda^4 < 1.15$	$-0.73 < F_{T,1}/\Lambda^4 < 0.72$	1.5
$-1.96 < F_{T,2}/\Lambda^4 < 1.85$	$-1.48 < F_{T,2}/\Lambda^4 < 1.37$	1.5
$-0.70 < F_{T,5}/\Lambda^4 < 0.74$	$-0.51 < F_{T,5}/\Lambda^4 < 0.57$	1.8
$-1.64 < F_{T,6}/\Lambda^4 < 1.67$	$-1.23 < F_{T,6}/\Lambda^4 < 1.26$	1.7
$-2.59 < F_{T,7}/\Lambda^4 < 2.80$	$-1.91 < F_{T,7}/\Lambda^4 < 2.12$	1.8
$-0.47 < F_{T,8}/\Lambda^4 < 0.47$	$-0.36 < F_{T,8}/\Lambda^4 < 0.36$	1.6
$-1.26 < F_{T,9}/\Lambda^4 < 1.27$	$-0.95 < F_{T,9}/\Lambda^4 < 0.95$	1.5

The unitarity bound is determined using the VBFNLO framework.

Great improvement compare to RunI's observed limits.

Better than current best limits on red-marked parameters

RunI's limits

Observed Limits
$-71\ (TeV^{-4}) < f_{M0}/\Lambda^4 < 75\ (TeV^{-4})$
$-190\ (TeV^{-4}) < f_{M1}/\Lambda^4 < 182\ (TeV^{-4})$
$-32\ (TeV^{-4}) < f_{M2}/\Lambda^4 < 31\ (TeV^{-4})$
$-58\ (TeV^{-4}) < f_{M3}/\Lambda^4 < 59\ (TeV^{-4})$
$-3.8\ (TeV^{-4}) < f_{T0}/\Lambda^4 < 3.4\ (TeV^{-4})$
$-4.4\ (TeV^{-4}) < f_{T1}/\Lambda^4 < 4.4\ (TeV^{-4})$
$-9.9\ (TeV^{-4}) < f_{T2}/\Lambda^4 < 9.0\ (TeV^{-4})$
$-1.8\ (TeV^{-4}) < f_{T8}/\Lambda^4 < 1.8\ (TeV^{-4})$
$-4.0\ (TeV^{-4}) < f_{T9}/\Lambda^4 < 4.0\ (TeV^{-4})$

Summary and outlook

- Results:
  - Observes(Expected) significance is 3.9(5.2)σ for EW Zγ with 2016 data only, 4.7(5.5)σ after combining 8 TeV results
  - fiducial cross-section measurement reported
  - dim-8 operator limits were shown, obtain several most constraint limits

- Outlook
  - Full runII analysis for EW Zγ is ongoing, an observation is very promising, and more measurements will be implemented.

Backup

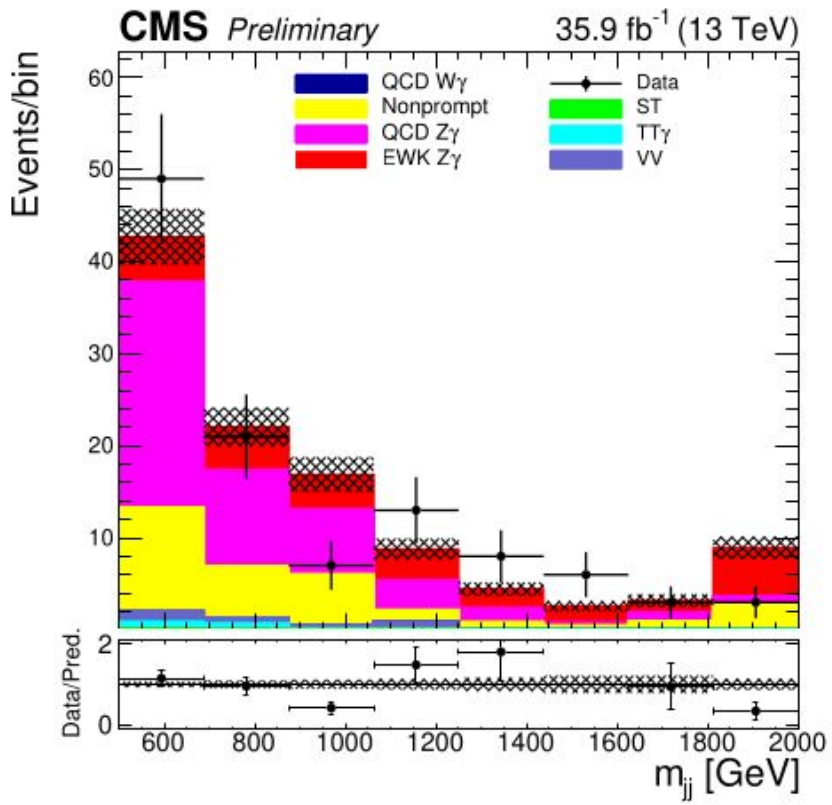

(a)

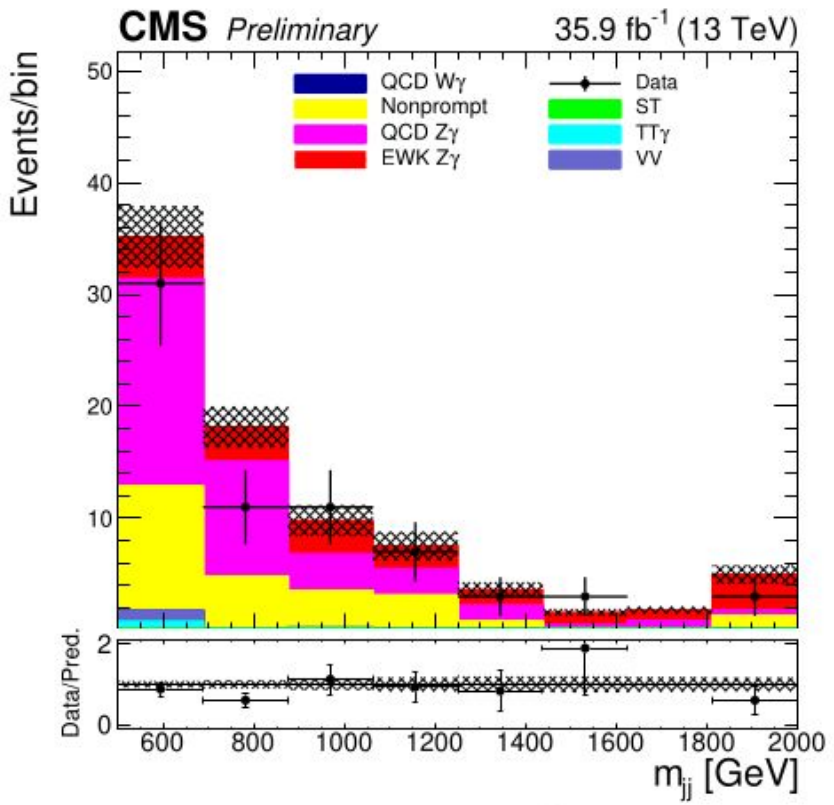

(b)

Figure 2: The m_{jj} distributions measured in the (left) dimuon plus barrel photon and (right) dielectron plus barrel photon categories. The data (solid symbols with error bars representing the statistical uncertainties) are compared to a data-driven background estimation, combined with MC predictions. The hatched bands represent the statistical uncertainty of the combined prediction of the signal and all of the backgrounds. The last bin includes overflow events.

L1 prefiring effect

In 2016 and 2017, the gradual timing shift of ECAL was not properly propagated to L1 trigger primitives (TP) resulting in a significant fraction of high eta TP being mistakenly associated to the previous bunch crossing. This effect is not described by the simulations. Official recipe have been provided.

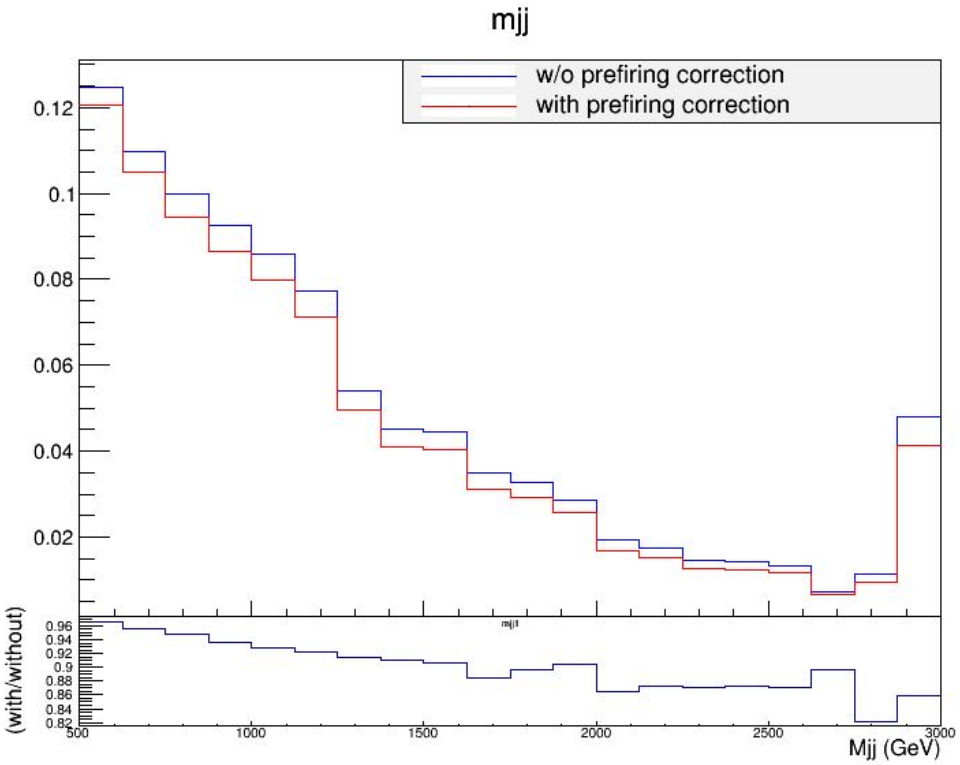

upward and downward values of the event weights are provided, propagated to signal region.

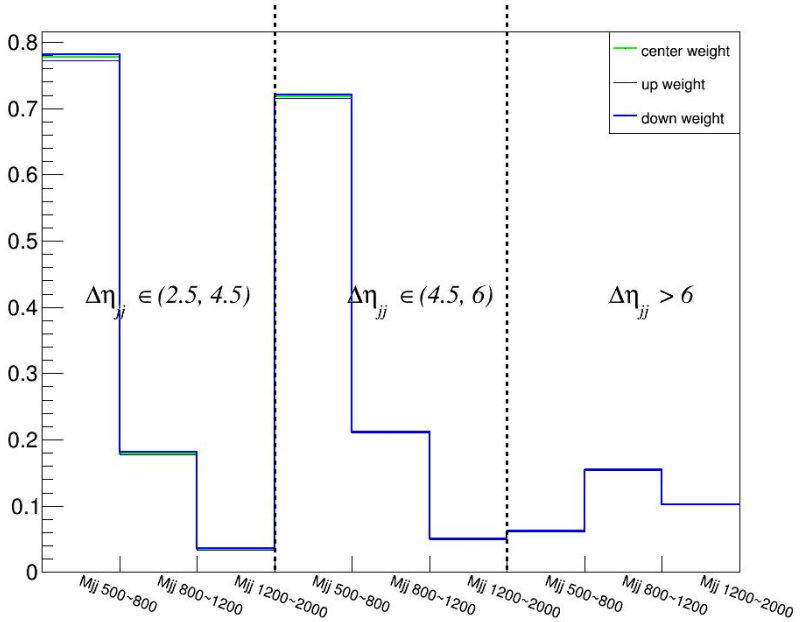

The correction have large effect on the results, thus updated results are shown in the next slides.

L1 prefiring effect

Consistent with the plot of EW W+jets (SMP-17-011)

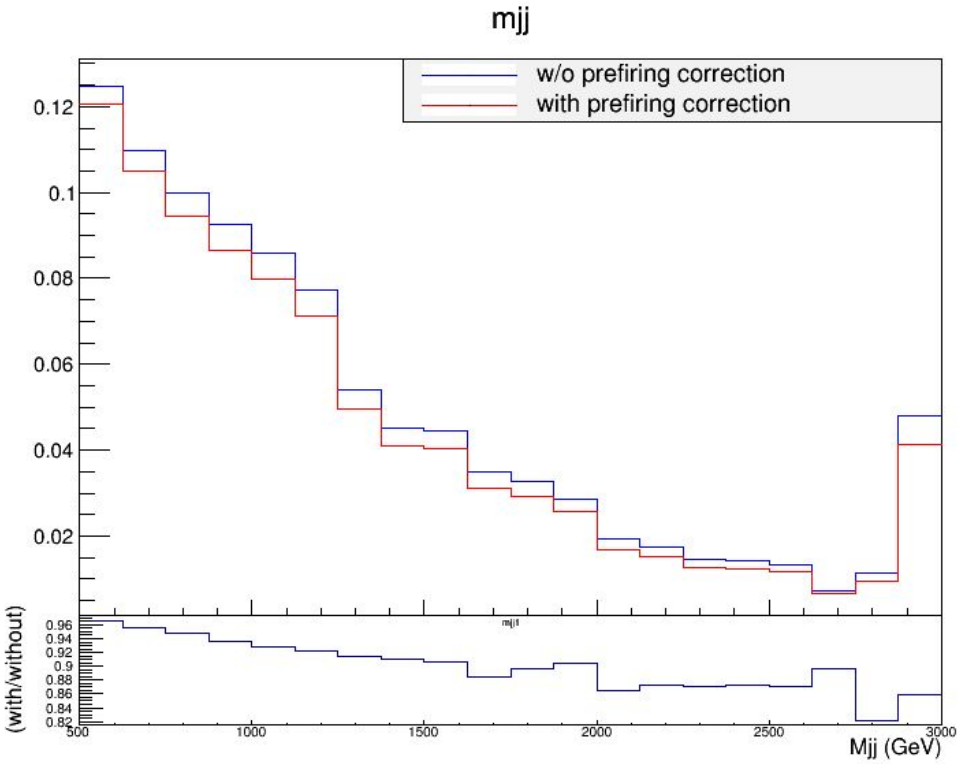

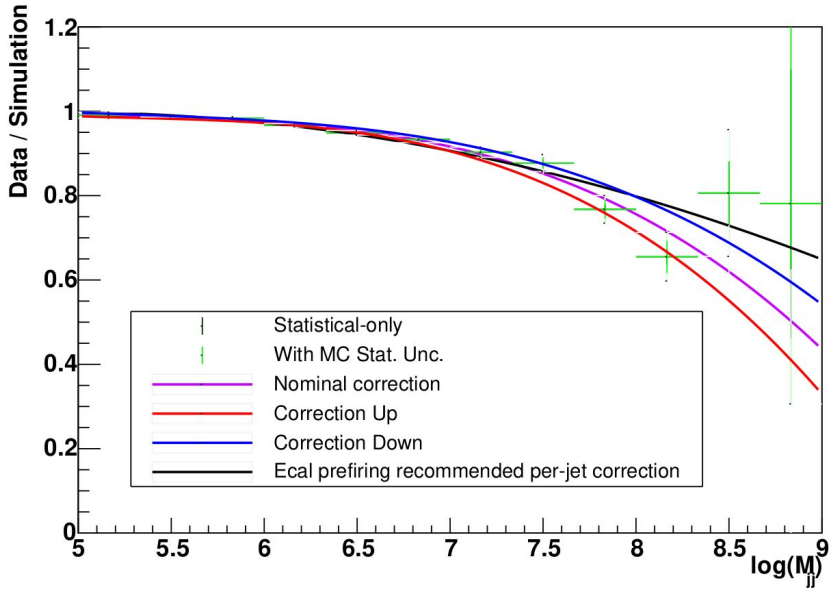

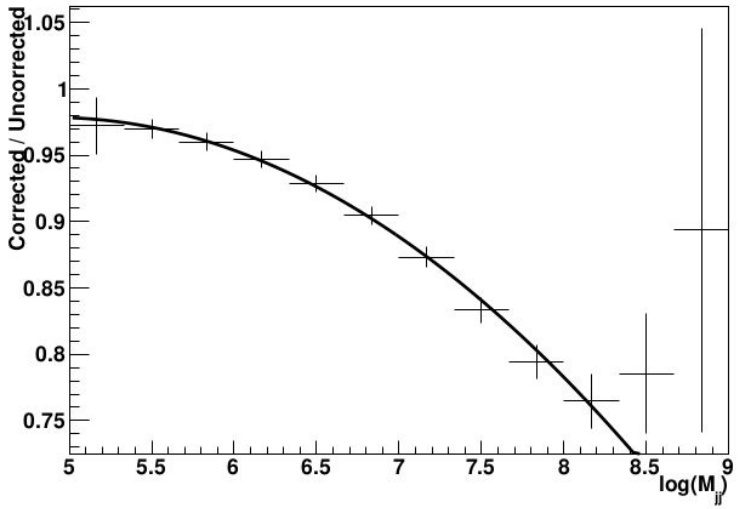

Fit result

Barrel region, 20 GeV < photon PT < 25 GeV

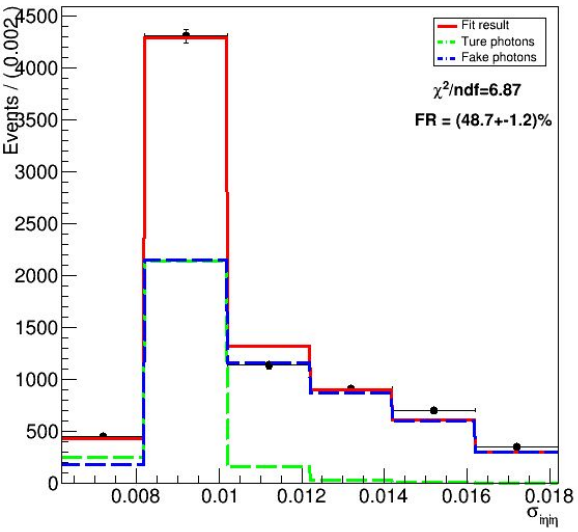

Barrel region, 25 GeV < photon PT < 30 GeV

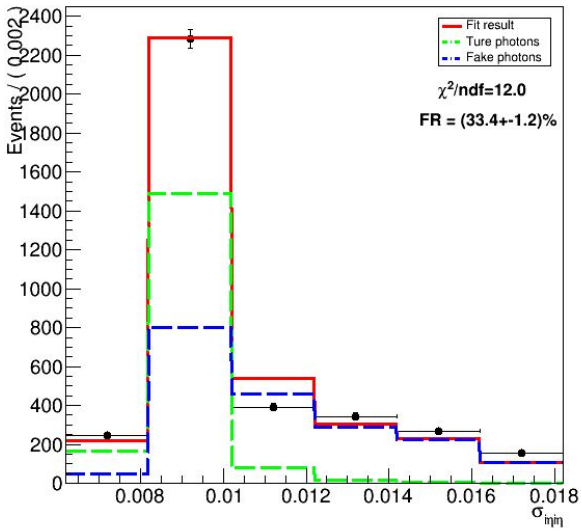

Barrel region, 30 GeV < photon PT < 35 GeV

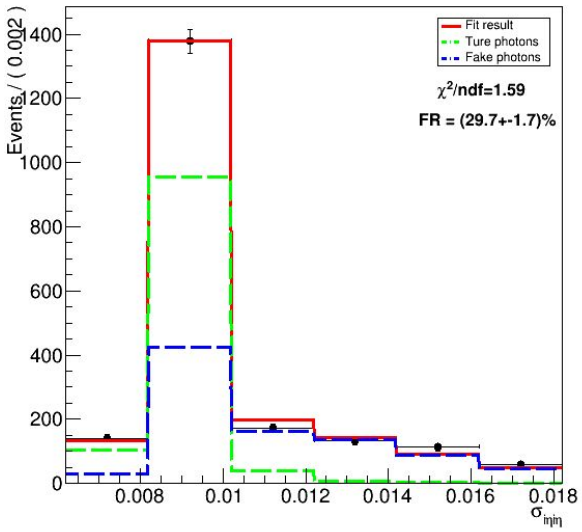

Barrel region, 35 GeV < photon PT < 40 GeV

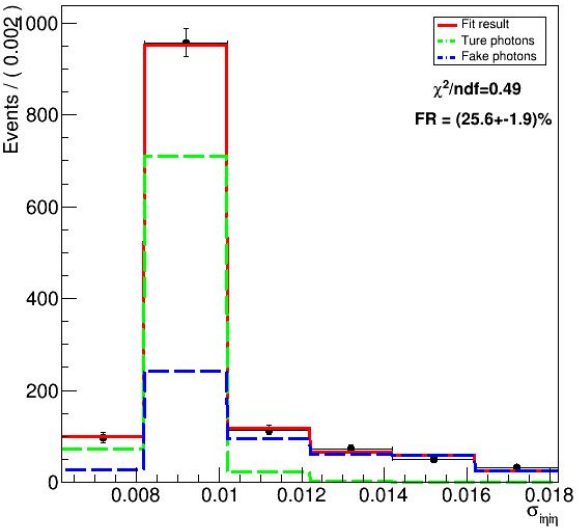

Barrel region, 40 GeV < photon PT < 45 GeV

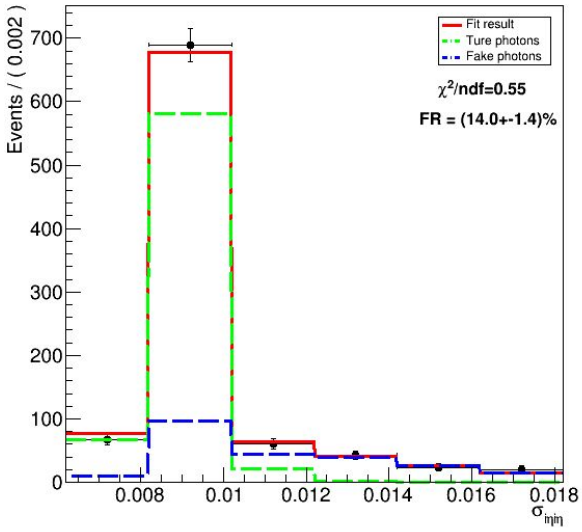

Barrel region, 45 GeV < photon PT < 50 GeV

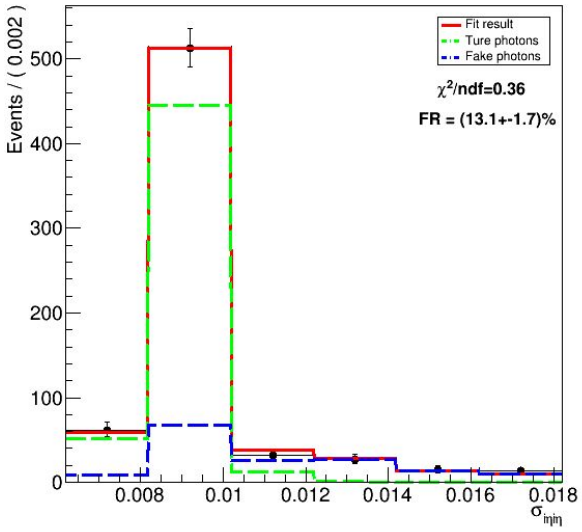

Fit result using different bin number

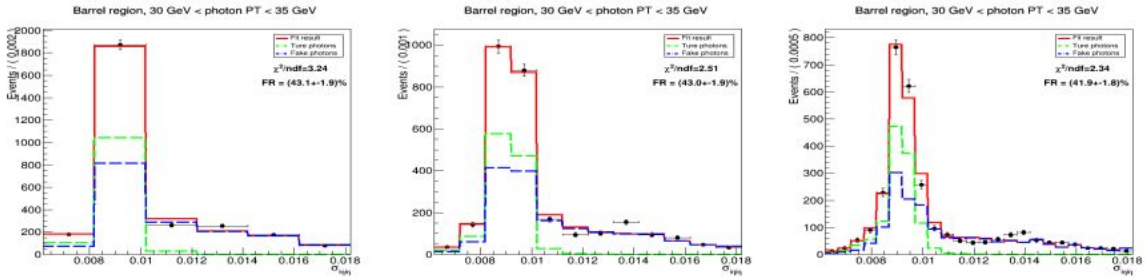

Figure 41: Template fit results for muon barrel channel for photon p_T bins 30 GeV to 35 GeV with 6bins, 12bins and 24bins.

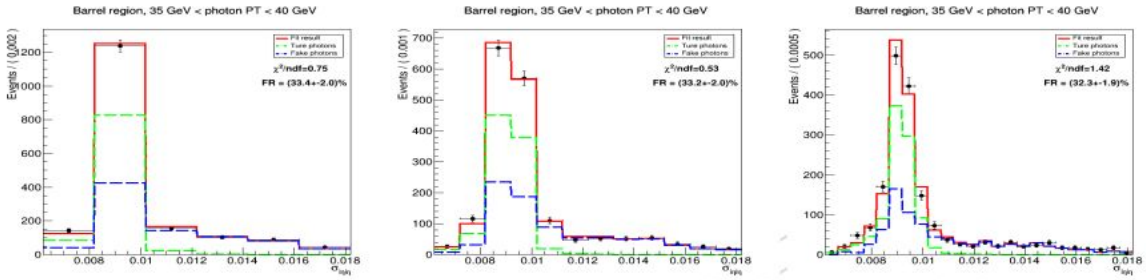

Figure 42: Template fit results for muon barrel channel for photon p_T bins 35 GeV to 40 GeV with 6bins, 12bins and 24bins.

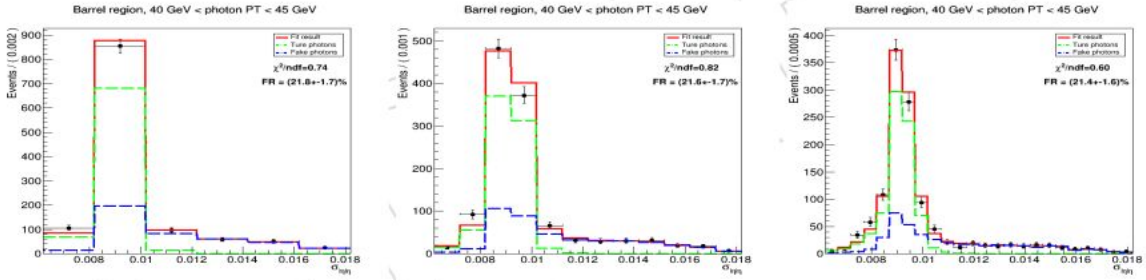

Figure 43: Template fit results for muon barrel channel for photon p_T bins 40 GeV to 45 GeV with 6bins, 12bins and 24bins.

Fake fraction is almost independent on the bin number used for fitting

Theoretical uncertainties

The largest uncertainties come from theoretical uncertainties.

PDF uncertainty: following PDF4LHC

$$\mathcal{O}_0 = \langle \mathcal{O} \rangle_{rep} = \frac{1}{N_{rep}} \sum_{j=1}^{N_\alpha} \sum_{k_j=1}^{N_{\mathrm{rep}}^{\alpha_s^{(j)}}} \mathcal{O}\left(\mathrm{PDF}^{(k_j,j)}, \alpha_s^{(j)}\right)$$

$$\sigma^{NNPDF}(\alpha_s + PDF) = \left[\frac{1}{N_{rep}-1} \sum_{j=1}^{N_\alpha} \sum_{k_j=1}^{N_{\mathrm{rep}}^{\alpha_s^{(j)}}} \left(\mathcal{O}\left(\mathrm{PDF}^{(k_j,j)}, \alpha_s^{(j)}\right) - \mathcal{O}_0\right)^2 \right]^{1/2}$$

Scale uncertainty

By varing μ_R and μ_F by factor 2 and 0.5, discarding the case where one scale is multiplied by 2 and the other by 0.5, 1 central weight and 6 variations.

σ_scale = max - min

Same methods are used for QCD Zγ and signal theoretical uncertainties estimation.

Fake photon uncertainties

Weights of events of PLJ sample: $W_{p_T^\gamma} = \frac{h_{data} \rightarrow GetBinContent(p_T^\gamma)}{h_{plj} \rightarrow GetBinContent(p_T^\gamma)} * fake\_fraction_{p_T^\gamma}$,

Uncertainties of fake fraction:

- Charged isolation sideband choice for fake photon template

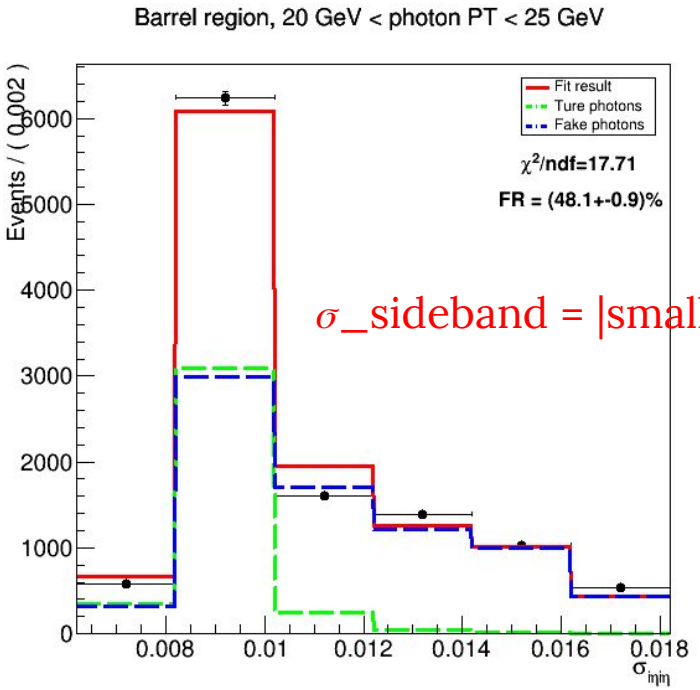

Smaller charged isolation sideband

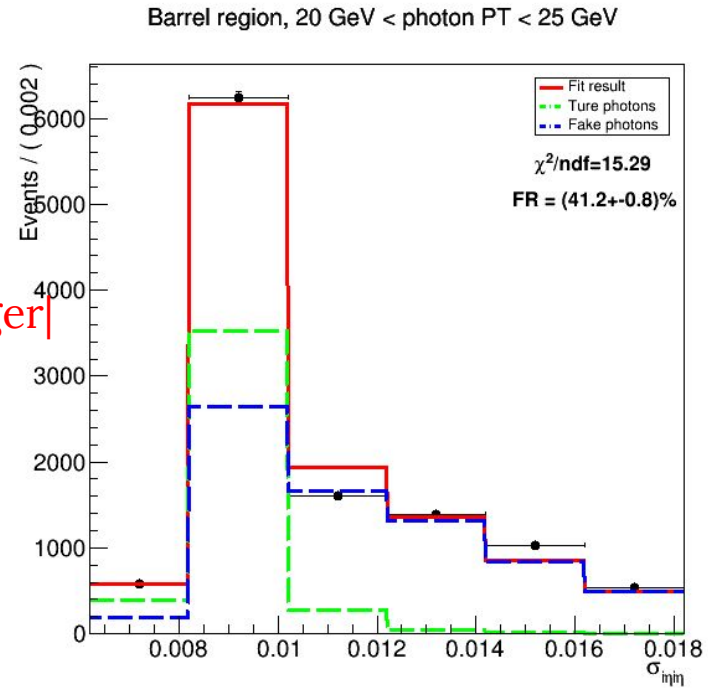

Larger charged isolation sideband

Fake photon uncertainties

Weights of events of PLJ sample: $W_{p_T^\gamma} = \frac{h_{data} \rightarrow GetBinContent(p_T^\gamma)}{h_{plj} \rightarrow GetBinContent(p_T^\gamma)} * fake\_fraction_{p_T^\gamma}$,

- Uncertainties of fake fraction:
- True template choice: can either choose QCD Zγ or signal sample to construct true photon template

σ_true = |EWK - QCD|

-

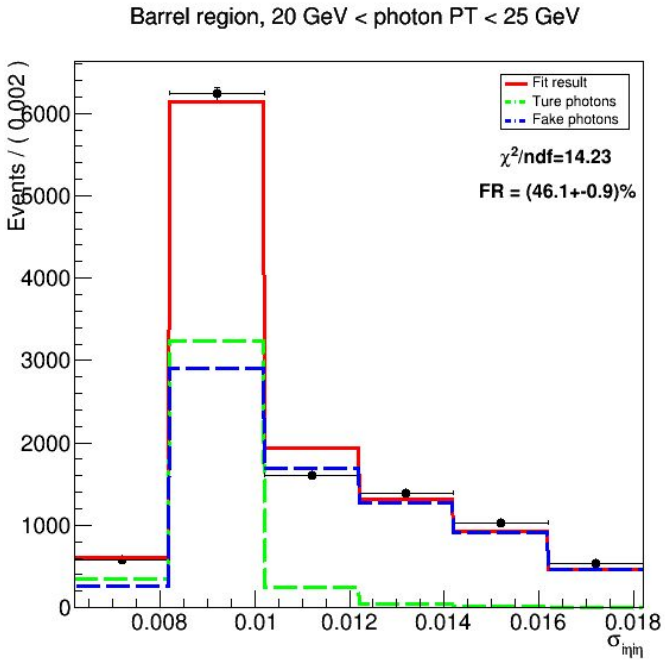

True template from signal sample

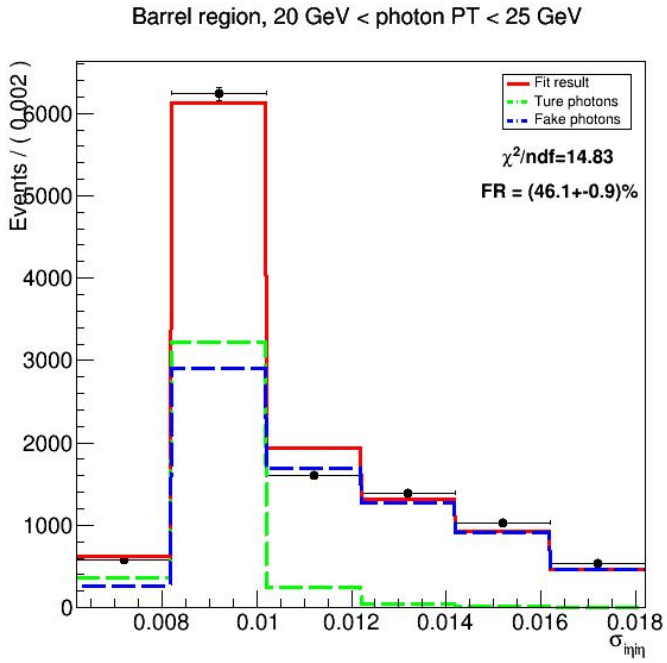

True template from QCD Zγ sample

Fake photon uncertainties

Weights of events of PLJ sample: $W_{p_T^\gamma} = \frac{h_{data} \rightarrow GetBinContent(p_T^\gamma)}{h_{plj} \rightarrow GetBinContent(p_T^\gamma)} * fake\_fraction_{p_T^\gamma}$,

Uncertainties of fake fraction:

- Closuretest uncertainty: using pseudo-data to perform template method. The difference between fake fraction from fitting and MC truth fake fraction, woulb be regarded as closuretest uncertainty.

σ_closuretest = |fit result - MC truth|

Combining all the three uncertainties, propagate fake fraction uncertainty to PLJ weights uncertainty.

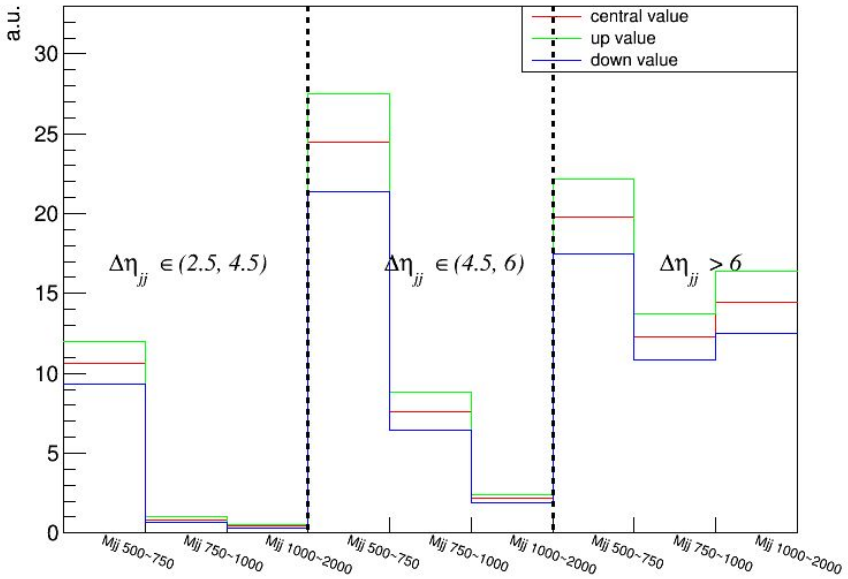

Interference between QCD/EWK Zγ

Using MG5 to study interference effect:

- EWK llγ+2jets: (QED=5, QCD=0)
- QCD llγ+2jets: (QED=3, QCD=2)
- EWK+QCD interference: (QED=4, QCD=1)

Interference uncertainty on signal:
σ_Interference = |EWK+QCD interference - EWK llγ+2jets - QCD llγ+2jets|/EWK llγ+2jets

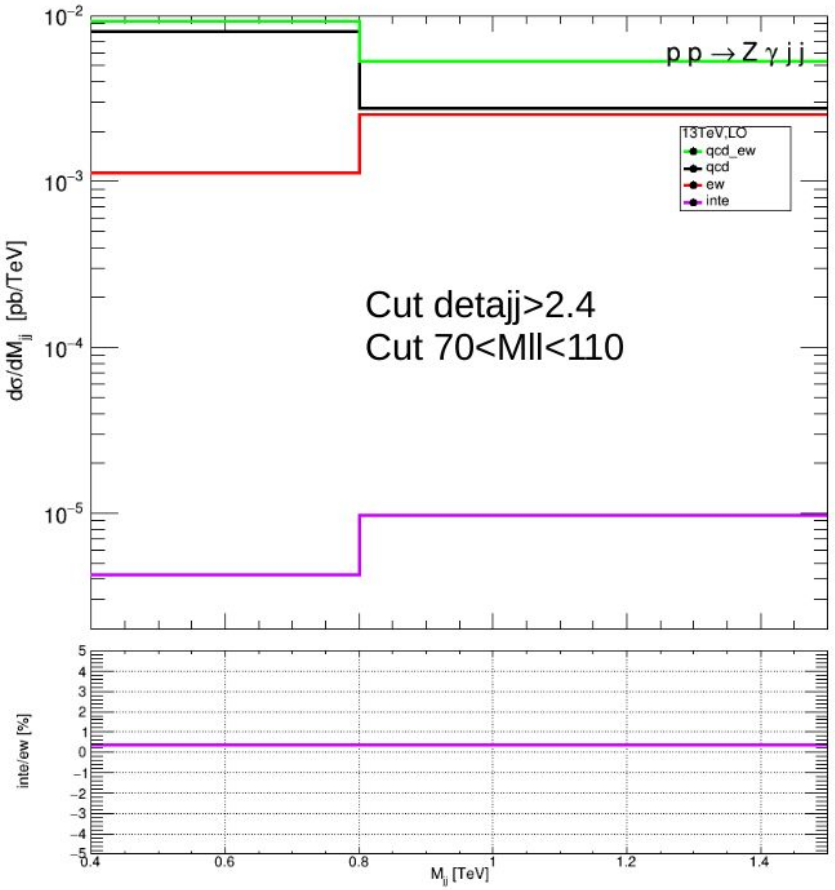

Jet energy correction and resolution uncertainty

- Jet energy correction: following twiki.
- Jet energy resolution: Measurements show that the jet energy resolution (JER) in data is worse than in the simulation and the jets in MC need to be smeared to describe the data. Following twiki.
- Checked with official reference table.
- Uncertainty is propagated to signal region w.r.t Mjj and detajj bins.

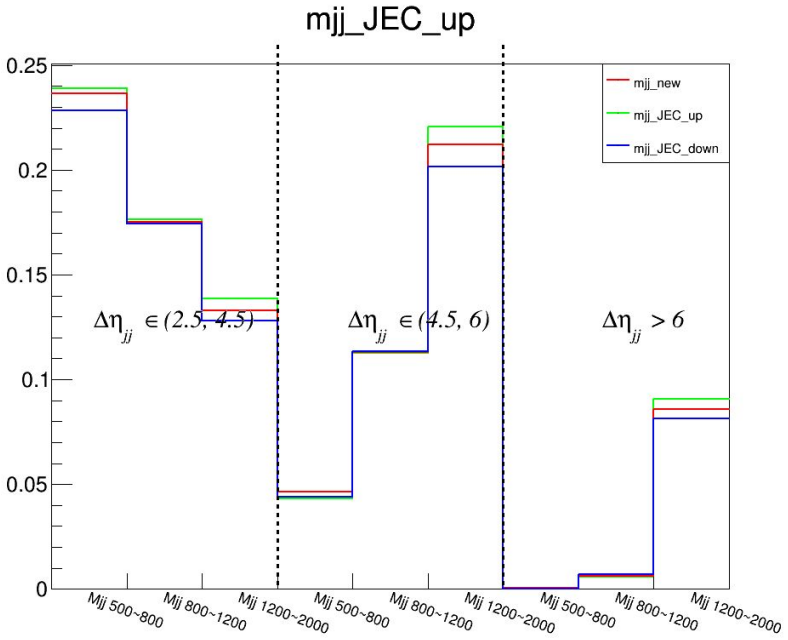

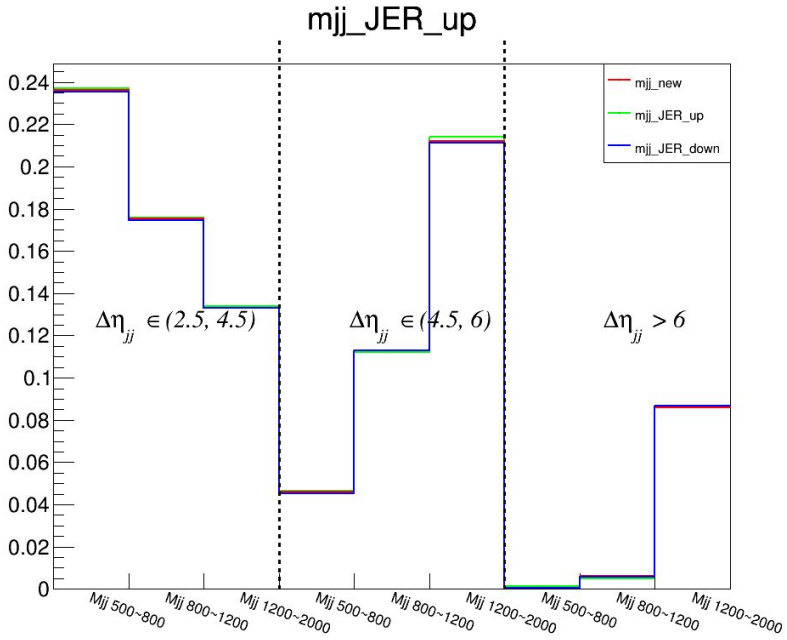

Uncertainty estimation: JERC

First do crosscheck with official twiki,
MC reference table:
MC:
/store/mc/RunIISpring16MiniAODv2/TT_TuneCUETP8M1_13TeV-powheg-pythia8/MINIAODSIM/PUSpring16_80X_mcRun2_asymptotic_2016_miniAODv2_v0_ext3-v2/70000/041A166C-B53F-E611-BF34-5CB90179CCC0.root
MC: 80X_mcRun2_asymptotic_2016_miniAODv2_v1

Reference table

Event	Jet #	p_T	η	Uncorrected p_T	Recorrected p_T (using new JEC)	Smeared p_T (jet smeared after new JEC)	JEC uncertainty (%)
1:26459:5269847	#1	139.964	0.65832	133.879	139.964	140.041	0.89024
	#2	64.0428	2.332	55.8187	64.0428	65.6575	1.98422
	#3	39.0866	-0.298268	37.8474	39.0866	38.2265	2.78979
	#4	18.0098	3.29539	18.0735	18.0098	19.4395	8.05295
	#5	14.2157	-1.14937	13.7436	14.2157	14.2708	5.90153
	#6	13.6179	-0.208815	13.3202	13.6179	13.9482	5.94856
	#7	11.872	5.01535	7.28939	11.872	11.872	8.87051
	#8	10.9012	1.19237	10.7343	10.9012	12.2209	7.06457
	#9	10.8789	0.77675	11.2231	10.8789	11.9521	6.77754
	#10	10.4956	-3.12483	11.104	10.4956	10.4956	10.8152
	#11	10.062	-0.0482175	10.3967	10.062	10.3092	7.203

My output

```
Begin processing the 1st record. Run 1, Event 5269847,
0.65832 133.879 139.964 140.041 0.0089024 141.495
2.332 55.8187 64.0428 65.6575 0.0198422 67.1417
-0.298268 37.8474 39.0866 38.2265 0.0278979 39.4499
3.29539 18.0735 18.0098 20.1707 0.0805295 22.296
-1.14937 13.7436 14.2157 14.2708 0.0590153 15.134
-0.208815 13.3202 13.6179 13.9482 0.0594856 14.8571
5.01535 7.28939 11.872 11.872 0.0887051 12.9251
1.19237 10.7343 10.9012 10.8449 0.0706457 11.6256
0.77675 11.2231 10.8789 9.43171 0.0677754 10.9719
-3.12483 11.104 10.4956 10.4956 0.108152 11.6307
-0.0482175 10.3967 10.062 10.3092 0.07203 11.1224
```

L1 prefiring effect

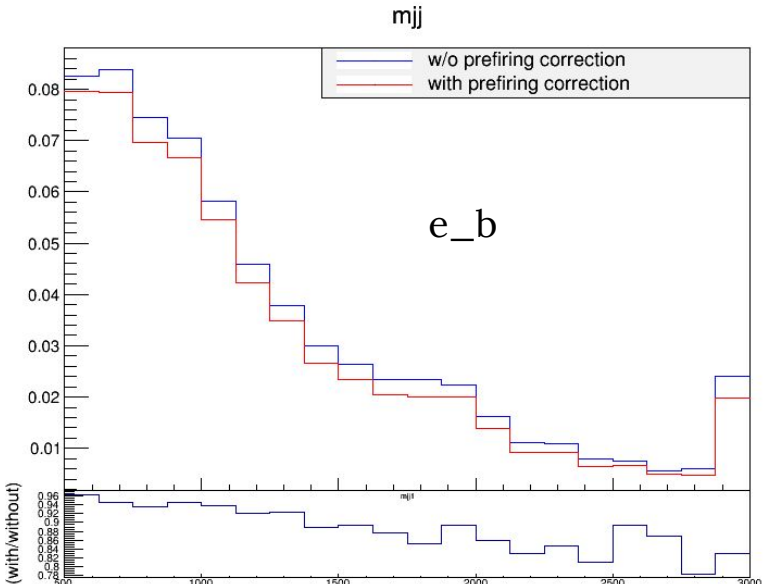

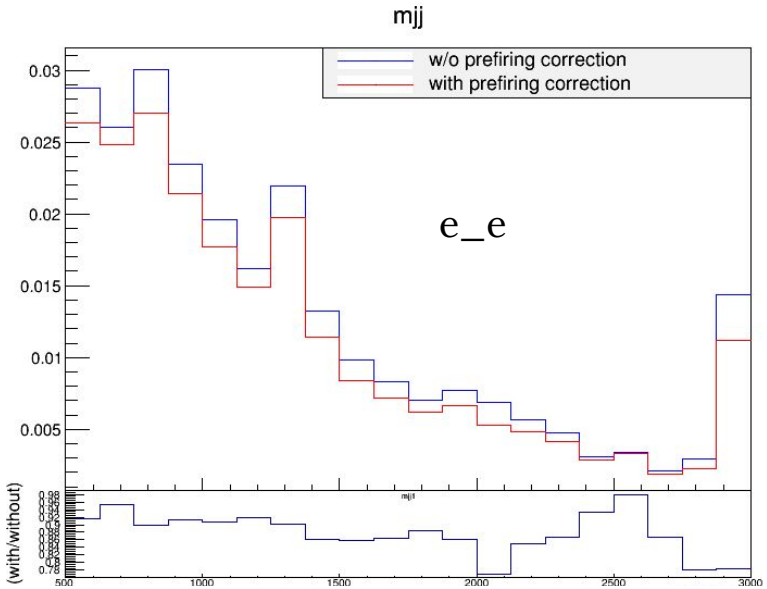

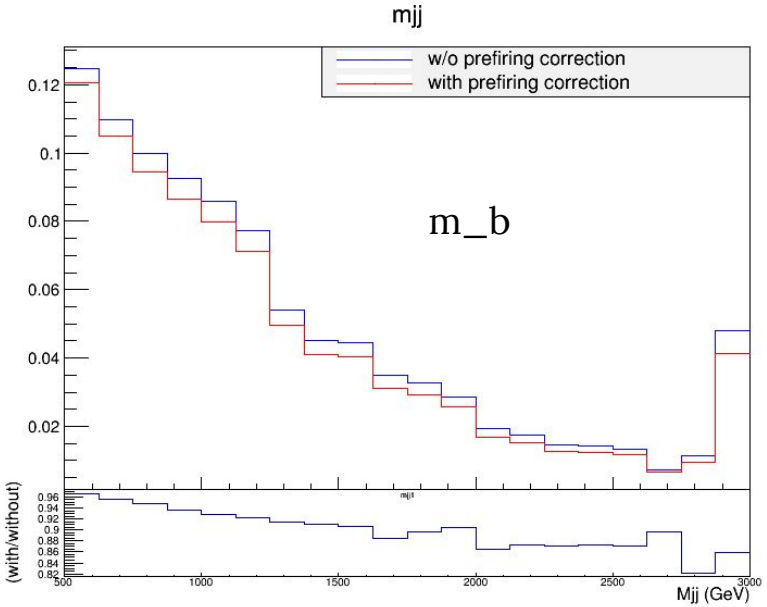

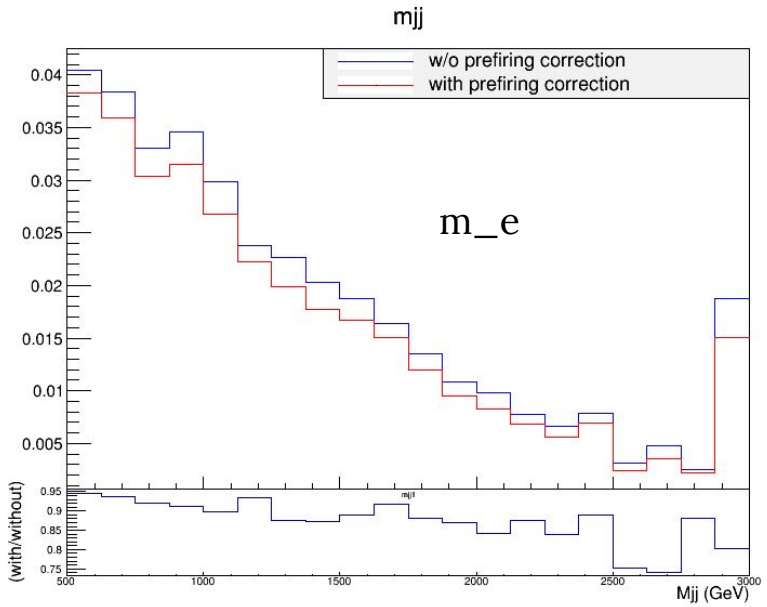

L1 prefiring effect in SMP-17-011

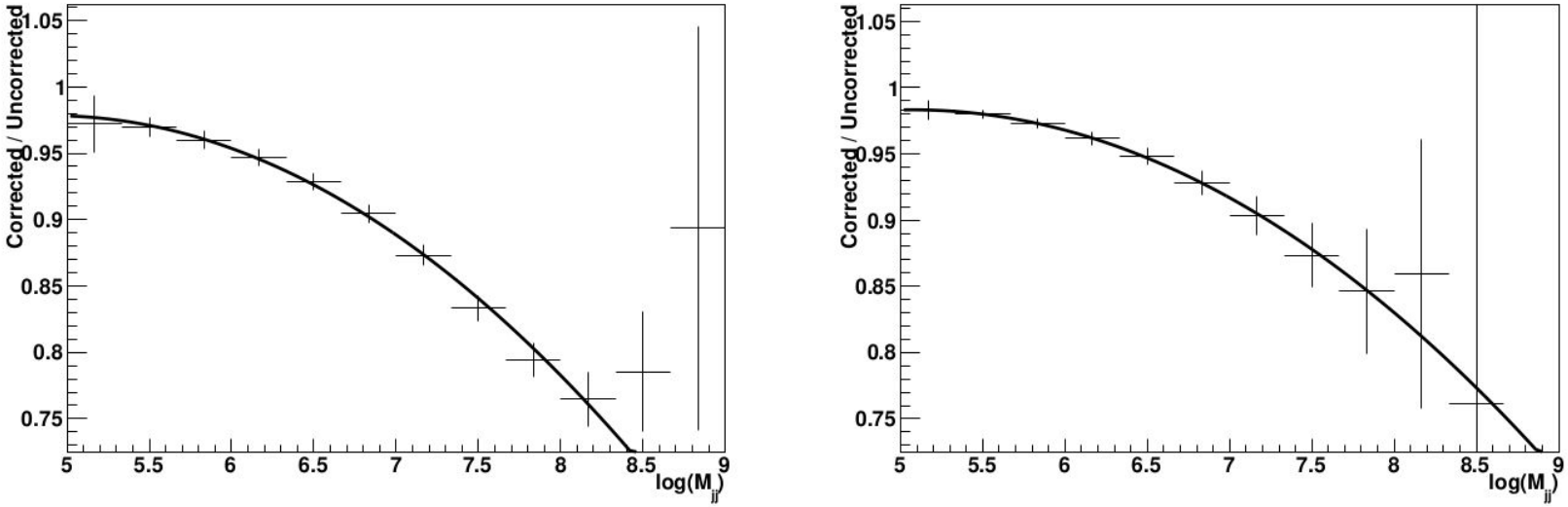

Figure 24: Effect of preliminary corrections for the L1 ECAL prefiring effect vs. log(M(jj)) for signal (left) and background (right).

aQGC estimation: expected limits

Without l1 prefiring

Expected Limits	Unitarity Bound
$-15.23\ (TeV^{-4}) < f_{M0}/\Lambda^4 < 15.30\ (TeV^{-4})$	1.0
$-30.46(TeV^{-4}) < f_{M1}/\Lambda^4 < 30.34\ (TeV^{-4})$	1.2
$-6.18\ (TeV^{-4}) < f_{M2}/\Lambda^4 < 6.15\ (TeV^{-4})$	1.3
$-13.30\ (TeV^{-4}) < f_{M3}/\Lambda^4 < 13.34\ (TeV^{-4})$	1.5
$-11.80\ (TeV^{-4}) < f_{M4}/\Lambda^4 < 11.80\ (TeV^{-4})$	1.5
$-19.19\ (TeV^{-4}) < f_{M5}/\Lambda^4 < 18.39\ (TeV^{-4})$	1.8
$-30.46\ (TeV^{-4}) < f_{M6}/\Lambda^4 < 30.58\ (TeV^{-4})$	1.0
$-46.41\ (TeV^{-4}) < f_{M7}/\Lambda^4 < 46.60\ (TeV^{-4})$	1.3
$-0.56\ (TeV^{-4}) < f_{T0}/\Lambda^4 < 0.51\ (TeV^{-4})$	1.4
$-0.73\ (TeV^{-4}) < f_{T1}/\Lambda^4 < 0.72\ (TeV^{-4})$	1.5
$-1.48\ (TeV^{-4}) < f_{T2}/\Lambda^4 < 1.38\ (TeV^{-4})$	1.5
$-0.51\ (TeV^{-4}) < f_{T5}/\Lambda^4 < 0.56\ (TeV^{-4})$	1.8
$-1.25\ (TeV^{-4}) < f_{T6}/\Lambda^4 < 1.28\ (TeV^{-4})$	1.7
$-1.91\ (TeV^{-4}) < f_{T7}/\Lambda^4 < 2.12\ (TeV^{-4})$	1.8
$-0.34\ (TeV^{-4}) < f_{T8}/\Lambda^4 < 0.34\ (TeV^{-4})$	1.6
$-0.92\ (TeV^{-4}) < f_{T9}/\Lambda^4 < 0.92\ (TeV^{-4})$	1.5

With l1 prefiring

Expected Limits	Unitarity Bound
$-15.29\ (TeV^{-4}) < f_{M0}/\Lambda^4 < 15.36\ (TeV^{-4})$	1.0
$-30.59(TeV^{-4}) < f_{M1}/\Lambda^4 < 30.47\ (TeV^{-4})$	1.2
$-6.21\ (TeV^{-4}) < f_{M2}/\Lambda^4 < 6.15\ (TeV^{-4})$	1.3
$-13.40\ (TeV^{-4}) < f_{M3}/\Lambda^4 < 13.42\ (TeV^{-4})$	1.5
$-11.85\ (TeV^{-4}) < f_{M4}/\Lambda^4 < 11.90\ (TeV^{-4})$	1.5
$-19.35\ (TeV^{-4}) < f_{M5}/\Lambda^4 < 18.47\ (TeV^{-4})$	1.8
$-30.59\ (TeV^{-4}) < f_{M6}/\Lambda^4 < 30.71\ (TeV^{-4})$	1.0
$-46.78\ (TeV^{-4}) < f_{M7}/\Lambda^4 < 47.14\ (TeV^{-4})$	1.3
$-0.56\ (TeV^{-4}) < f_{T0}/\Lambda^4 < 0.51\ (TeV^{-4})$	1.4
$-0.73\ (TeV^{-4}) < f_{T1}/\Lambda^4 < 0.72\ (TeV^{-4})$	1.5
$-1.49\ (TeV^{-4}) < f_{T2}/\Lambda^4 < 1.38\ (TeV^{-4})$	1.5
$-0.52\ (TeV^{-4}) < f_{T5}/\Lambda^4 < 0.57\ (TeV^{-4})$	1.8
$-1.25\ (TeV^{-4}) < f_{T6}/\Lambda^4 < 1.28\ (TeV^{-4})$	1.7
$-1.92\ (TeV^{-4}) < f_{T7}/\Lambda^4 < 2.14\ (TeV^{-4})$	1.8
$-0.34\ (TeV^{-4}) < f_{T8}/\Lambda^4 < 0.34\ (TeV^{-4})$	1.6
$-0.93\ (TeV^{-4}) < f_{T9}/\Lambda^4 < 0.93\ (TeV^{-4})$	1.5

L1 prefiring has very small effect on aQGC limits

Current aQGC limits

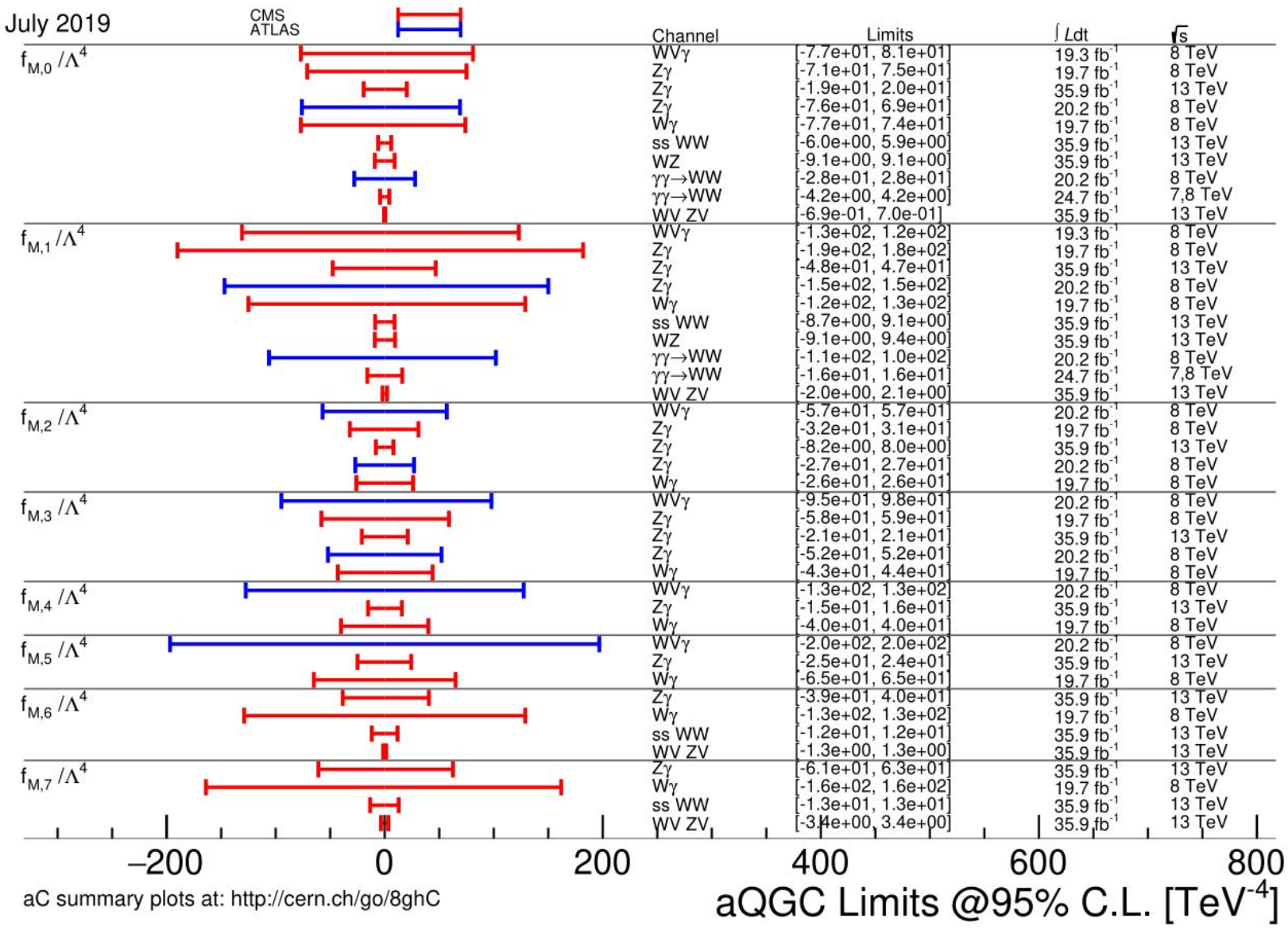

Current aQGC limits